

Relativistic treatment of the charged-current reaction $^{12}\text{C}(\nu_\mu, \mu^-)$ near threshold

Hungchong Kim ^{1*}, J. Piekarewicz ^{2 †}, C. J. Horowitz ^{1 ‡}

¹ *Nuclear Theory Center and Dept. of Physics, Indiana University, Bloomington, Indiana 47408*

² *Supercomputer Computations Research Institute, Florida State University,
Tallahassee, Florida 32306*

Abstract

We compute the cross section for the charged-current reaction $^{12}\text{C}(\nu_\mu, \mu^-)$ near threshold using a relativistic mean-field formalism. A reduced value of the nucleon mass in the medium — coupled to the finite muon mass — leads to a 30% reduction in the cross section relative to a free Fermi-gas estimate. Isovector RPA correlations, which are strongly repulsive at these momentum transfers, reduce the cross section by an additional 15-30%. Hence, relativistic nuclear-structure effects can account for the more than a factor-of-two reduction in the cross section recently reported by the LSND collaboration.

PACS number(s): 25.30.Pt, 24.10.Jv, 21.60.Jz

Typeset using REVTeX

*Email: hung@iucf.indiana.edu

†Email: jorgep@scri.fsu.edu

‡Email: charlie@iucf.indiana.edu

The remarkable achievements made over the past few years in neutrino-nucleus scattering are challenging our theoretical understanding of these reactions [1–4]. These processes, which complement electron-scattering studies, can broaden our understanding of nuclear structure and constitute a fruitful ground for testing the electroweak sector of the standard model. For example, charged-current neutrino (ν, μ) scattering experiments at high momentum transfer have been used to determine the axial form factor of the nucleon [5]. This knowledge, important in its own right, becomes essential for a reliable extraction of the strange-quark content of the nucleon from neutral-current neutrino (ν, p) scattering experiments. Indeed, the strong correlation between the axial mass parameter, M_A , and the isoscalar strange-form factor, g_A^s , complicates the extraction of strange-quark information [6,7]. Although the common assumption made to extract hadronic-structure information — that nuclear-structure effects can be described by a Fermi-gas response — seems justified at high momentum transfer, we have recently reported a 10% uncertainty in the extracted value of M_A due to nuclear-structure effects [8]. This uncertainty is so large that present-day experiments provide no significant evidence in favor of a nonzero g_A^s .

If nothing else, nuclear-structure effects will become more important at low-momentum transfers. Here Pauli blocking, binding-energy corrections, and RPA correlations — all unimportant at high momentum transfer — must be carefully addressed. Moreover, low-energy neutrino experiments open a new window into the study of the nuclear axial response. The axial response is not accessible with electromagnetic probes, yet it is as fundamental as the vector (longitudinal and transverse) responses measured in electron scattering. In addition, these reactions represent an important diagnostic tool for neutrino detection. Hence, the identification of novel and interesting physics — such as neutrino oscillation — becomes strongly coupled to the study of these inclusive reactions.

Motivated by recent experiments we devote this letter to the study of the charged-current reaction $^{12}\text{C}(\nu_\mu, \mu^-)$ near threshold [2,4]. We place particular emphasis on relativistic nuclear-structure effects in the hope of understanding the factor-of-two reduction in the inclusive cross section, relative to a Fermi-gas estimate, reported recently by the Liquid Scintillator Neutrino Detector (LSND) collaboration at LAMPF [4].

We have calculated the inclusive charged-current cross section using a relativistic mean-field approximation to the Walecka model [9,10]. The model is characterized by the presence of strong scalar and vector mean fields which induce large shifts in the mass (M^*) and energy of a nucleon in the medium. We use the impulse approximation to write the charged-current operator for a target nucleon in terms of single-nucleon form factors parameterized from on-shell data:

$$\Gamma^\mu(q) = F_1(Q^2)\gamma^\mu + iF_2(Q^2)\sigma^{\mu\nu}\frac{q_\nu}{2M} - G_A(Q^2)\gamma^\mu\gamma^5 + F_p(Q^2)q^\mu\gamma^5 \quad , \quad (Q^2 \equiv \mathbf{q}^2 - q_0^2) . \quad (1)$$

The nuclear-structure information is contained in a large set of nuclear response functions that are computed in nuclear matter using a relativistic random-phase approximation (RPA) to the Walecka model. A detailed account of the model can be found in Ref. [8]

At this point it is instructive to discuss our nuclear-matter approximation. From previous electron-scattering studies we know that a nuclear-matter response at small momentum transfers ($|\mathbf{q}| < 2k_F$) leads to an unrealistic distribution of quasielastic strength. Undoubtedly, our present neutrino calculations will suffer from the same deficiencies. Indeed, the “triangle-shaped” responses of Fig. 1 — which characterize any nuclear-matter calculation —

clearly display some of these limitations. Still, nuclear-matter calculations can be quite valuable. This value stems from the fact that present day neutrino experiments are still unable to map out the full distribution of quasielastic strength and, thus, are forced to combine many different measurements into an integrated cross section. By doing this, most of the fine details of the response are lost. It is clear, however, that with the emergence of more sophisticated experimental facilities and techniques finite-nucleus calculations will become imperative.

In order to understand the interplay between the different contributions to the inclusive cross section we have plotted in Fig. 1 the distribution of quasielastic strength, $d^2\sigma/dE_\mu d\Omega$, using the flux-weighted average neutrino energy for the LSND experiment, $E_\nu = 180$ MeV, and a characteristic momentum transfer of $|\mathbf{q}| = 210$ MeV. We have modeled the ground state of ^{12}C as a Fermi gas of nucleons, with mass M or M^* , at a Fermi momentum of $k_F = 225$ MeV. The relativistic Fermi gas result (impulse with M) is indicated with the solid line. For the most part, Fermi motion is responsible for a simple redistribution of single-particle strength. However, for the present kinematical conditions ($|\mathbf{q}| < 2k_F$) almost 35% of phase space is unavailable due to Pauli blocking. This suppression of the nuclear response, in conjunction with some kinematical constraints, generates a reduction of almost 50% in the cross section relative to its single-nucleon value.

Although interesting, the main focus of the present paper is not the Pauli suppression of the Fermi-gas cross section. Rather, it is how additional nuclear structure effects, such as those arising from a reduced nucleon mass and RPA correlations, induce a large reduction in the cross section relative to its Fermi-gas value. In this regard, it is particularly interesting to study the interplay between the effective nucleon mass M^* and the finite muon mass. Thus, we start with some simple kinematical considerations. First, the kinematical constraint, $|\mathbf{q}| \leq (E_\nu + |\mathbf{k}'_j|)$, imposed at the leptonic vertex leads to a maximum allowed value for the energy loss satisfying (for $E_\nu = 180$ MeV)

$$q^0 \leq E_\nu - \sqrt{(|\mathbf{q}| - E_\nu)^2 + m_j^2} = \begin{cases} 70.17 \text{ MeV,} & \text{for muons;} \\ 150.0 \text{ MeV,} & \text{for electrons.} \end{cases} \quad (2)$$

Note, the subscript j on the lepton momentum, $|\mathbf{k}'_j|$, represents either a muon or an electron. An additional constraint on q^0 can be obtained from examining the hadronic vertex. In this case the maximum allowed value corresponds to the energy transfer to a nucleon at the Fermi surface moving in the direction of the momentum transfer \mathbf{q} , i.e.,

$$q^0 \leq \sqrt{(k_F + |\mathbf{q}|)^2 + M^2} - \sqrt{k_F^2 + M^2} = \begin{cases} 69.29 \text{ MeV,} & \text{for } M^*/M = 1; \\ 95.67 \text{ MeV,} & \text{for } M^*/M = 0.68. \end{cases} \quad (3)$$

Note that both conditions must be simultaneously satisfied. Among the simplest consequences of a reduced nucleon mass is a shift in the position of the peak and an increase in the width of the quasielastic region. Indeed, these features are clearly visible in the impulse with M^* calculation (dot-dashed line in Fig. 1) where the position of the peak and the width of the quasielastic region have been scaled by roughly M/M^* . Note, however, that in the muon case the quasielastic strength is not exhausted because of the kinematical cutoff imposed by the finite muon mass. In particular, the interplay between M^* and the muon mass, together with other dynamical effects to be discussed shortly, generate a reduction of almost 30% in the integrated cross section relative to the Fermi-gas value (see Table I).

For comparison, the reduction in the electron case, where the full quasielastic strength is exhausted, becomes only 15% [see Fig. 1 (b) and Table I]. This 15% reduction is associated with the quenching — due to M^* — of the individual nuclear responses. A particularly interesting case is the largely untested axial response. This response is proportional to the imaginary part of the axial polarization defined by:

$$i\Pi^{\mu 5; \nu 5}(q) = \int \frac{d^4 p}{(2\pi)^4} \text{Tr}[G(p+q) \gamma^\mu \gamma^5 G(p) \gamma^\nu \gamma^5], \quad (4)$$

where $G(p)$ is the nucleon propagator. After some simple manipulations one can rewrite the axial polarization in terms of the vector polarization $\Pi^{\mu\nu}$, which is probed in electron scattering, and a leftover piece, i.e.,

$$\Pi^{\mu 5; \nu 5}(q) = \Pi^{\mu\nu}(q) + g^{\mu\nu} \Pi_A(q). \quad (5)$$

Since the vector current is conserved, i.e., $q_\mu \Pi^{\mu\nu} = \Pi^{\mu\nu} q_\nu = 0$, the violation of the axial current is reflected by the appearance of Π_A . Moreover, because this violation arises exclusively due to the presence of a mass term, Π_A must, then, be proportional to the nucleon mass. Hence, an in-medium reduction of the nucleon mass generates a corresponding reduction in this part of the response. In summary, about 15% of the quenching observed in the impulse with M^* calculation is due to a dynamical reduction of the nuclear response. The additional 15% — present only in the muon case — is due to the interplay between M^* and the finite muon mass.

Repulsive RPA correlations are responsible for an additional, and substantial, quenching of the cross section. We have adopted a conventional residual interaction consisting of $\pi + \rho + g'$ contributions [8]. At these low momentum transfers the longitudinal (pion-like) component of the residual interaction has barely become attractive while the transverse (rho-like) component remains large and repulsive. A repulsive interaction of this kind quenches the nuclear response and shifts quasielastic strength towards high-excitation energy (hardening). Note, the quenching and hardening of the transverse response measured in quasielastic electron scattering is well documented in the literature [11]. This quenching and hardening of the response is clearly observed in Fig. 1. For example, the position of the quasielastic peak in the RPA with M calculation (long-dashed lines) has been shifted by more than 30 MeV and the integrated strength reduced by almost 40% relative to the Fermi-gas values. The RPA reduction in the M^* case (short dashed line) is even more dramatic — particularly in the muon case. Since the repulsive RPA correlations shift strength towards high-excitation energy, the cutoff induced by the finite muon mass now removes a substantial part of the quasielastic strength — reducing the integrated cross section to only 36% of its Fermi-gas value [see Table I under RPA(I)]. Note that this value is considerably larger (57%) in the electron case.

In a recent publication [12] we have argued in favor of a residual interaction with a transverse component less repulsive than the one traditionally employed in nonrelativistic calculations and the one adopted by us, until now. We have indicated that, because of the in-medium reduction of the nucleon mass, a relativistic mean-field (impulse with M^*) calculation could account for most of the features (i.e., quenching and hardening) observed experimentally in the (e, e') transverse response without the need for such a repulsive residual interaction. Moreover, with this residual interaction we were able to reproduce most of the

spin observables measured in a recent quasielastic (\vec{p}, \vec{n}) experiment [13,14]. Our results with this residual interaction have been plotted with dots in Fig. 1. As expected from a less repulsive interaction the quenching of the cross section is not as large as before. Still, even in this case the integrated cross section amounts, in the muon case, to only 53% of its Fermi-gas value [see Table I under RPA(II)]. As before, this number grows considerably, up to 71%, in the electron case.

One can extend the calculation to other values of the momentum transfer in the hope of mapping out the two dimensional nuclear-response surface. This kind of analysis, which is now commonplace in electron-scattering, is at present not available with weak probes due to the low count rate of the reaction. Therefore, in an attempt to improve statistics present-day experiments combine many of these measurements into an integrated cross section. Moreover, since most of the neutrinos are produced from the decay of pions in flight one integrates over the experimental neutrino spectrum. In this way, many of the detailed features that one could in principle map out are, unfortunately, lost. Yet, some interesting properties remain. In Fig. 2 we report the angle-integrated cross section, $d\sigma/dE_\mu$, folded over the LSND neutrino spectrum $\phi(E_\nu)$, i.e.,

$$\left\langle \frac{d\sigma}{dE_\mu} \right\rangle = \frac{\int_0^\infty \frac{d\sigma}{dE_\mu} \phi(E_\nu) dE_\nu}{\int_0^\infty \phi(E_\nu) dE_\nu}, \quad (6)$$

where the above integrations have been carried out using the full range of the experimental spectrum, i.e., $0 \leq E_\nu \leq 300$ MeV. Note that the numerator has support only above the threshold value for the $^{12}\text{C}(\nu_\mu, \mu^-)$ reaction, or $E_\nu = 111.6$ MeV in the Fermi gas model.

The fact that all the models display a common spectral shape is an indication that most of the fine details present in the double-differential cross section have been lost. Yet, the large quenching still remains. Indeed, the quenching in the total inclusive cross section is almost identical to the one reported in Table I, i.e.,

$$\frac{\langle \sigma \rangle}{\langle \sigma_{FG} \rangle} = \begin{cases} 0.70(0.80), & \text{for impulse with } M^*; \\ 0.53(0.59), & \text{for RPA(I) with } M; \\ 0.39(0.51), & \text{for RPA(I) with } M^*; \\ 0.55(0.66), & \text{for RPA(II) with } M^*. \end{cases} \quad (7)$$

Here the numbers in parentheses are the appropriate ratios for electron neutrinos. Note that the flux-averaged inclusive cross section in the Fermi-gas limit is $\langle \sigma_{FG} \rangle = 8.11 \times 10^{-40} \text{cm}^2$ for muons and $\langle \sigma_{FG} \rangle = 23.13 \times 10^{-40} \text{cm}^2$ for electrons. Thus, the the flux-averaged inclusive cross section in the RPA(I) with M^* model is only $\langle \sigma \rangle = 3.16 \times 10^{-40} \text{cm}^2$, or 0.39 of its Fermi gas value, in the muon case. Note, these cross sections were computed without Coulomb corrections.

In summary, we have calculated the charged-current reaction $^{12}\text{C}(\nu_\mu, \mu^-)$ near threshold in a relativistic formalism. We have incorporated nuclear-structure corrections arising from an in-medium reduction of the nucleon mass and RPA correlations. The reduction of the nucleon mass coupled to the finite muon mass prevents the quasielastic strength from being exhausted and results in a 30% quenching of the inclusive cross section relative to a Fermi-gas estimate. Repulsive RPA correlation exacerbate the effect and, depending on the form of the residual interaction, give rise to a reduction in the cross section anywhere from 45-60%.

Thus, relativistic nuclear-structure effects seem to be able to account for the factor-of-two reduction in the cross section reported by the LSND collaboration.

The large reductions, relative to a free Fermi gas, seen in the LSND experiment and our calculations may have important implications for atmospheric neutrino detection. Presently there is an anomaly in the observed ratio of atmospheric neutrinos, ν_μ/ν_e , which could signal neutrino oscillations [15]. Although the atmospheric spectrum is typically more energetic than LSND, the average nuclear excitation energy and momentum transfer are still modest. Therefore we find that our relativistic nuclear-structure effects may still be significant for atmospheric neutrinos. In a future work we will study how these effects change: (1) the absolute μ or e cross section, (2) the energy dependence of the μ quasielastic cross section and (3) the ratio of μ to e cross sections.

ACKNOWLEDGMENTS

This research was supported by the U.S. Department of Energy through contracts # DE-FG02-87ER40365, DE-FC05-85ER250000, and DE-FG05-92ER40750.

REFERENCES

- [1] R.C. Allen *et al.*, Phys. Rev. Lett. **64**, 1871 (1990).
- [2] D.D. Koetke *et al.*, Phys. Rev. C **46**, 2554 (1992).
- [3] B. Bodmann *et al.*, Nucl. Phys. **A553**, 831c (1993).
- [4] M. Albert *et al.*, LANL Bulletin Board preprint # nucl-th-9410039.
- [5] L. A. Ahrens *et al.*, Phys. Lett. **B202**, 284 (1988).
- [6] G.T. Garvey, W.C. Louis and D.H. White Phys. Rev. C **48**, 761 (1993).
- [7] C.J. Horowitz, Hungchong Kim, D. Murdock, and S. Pollock, Phys. Rev. C **48**, 3078 (1993).
- [8] Hungchong Kim, J. Piekarewicz, and C.J. Horowitz, *submitted to* Phys. Rev. C; LANL Bulletin Board preprint # nucl-th-9412017.
- [9] J.D. Walecka, Ann. Phys. **83**, 491 (1974).
- [10] B.D. Serot and J.D. Walecka, Adv. in Nucl. Phys. **16**, J.W. Negele and E. Vogt, eds. (Plenum, N.Y. 1986).
- [11] W.M. Alberico, M. Ericson and A. Molinari, Nucl. Phys. **A379**, 429 (1982).
- [12] C.J. Horowitz and J. Piekarewicz, Phys. Lett. **B301**, 321 (1993); Phys. Rev. C **50**, 2540 (1994).
- [13] J.B. McClelland *et al.*, Phys. Rev. Lett. **69**, 582 (1992).
- [14] X.Y. Chen *et al.*, Phys. Rev. C **47**, 2159 (1993).
- [15] K. S. Hirata *et al.*, Phys. Lett. **B280**, 146 (1992); K. S. Hirata *et al.*, Phys. Lett. **B205**, 416 (1988); E. W. Beier *et al.*, Phys. Lett. **B283**, 446 (1992).

FIGURES

FIG. 1. Double-differential cross section for the $^{12}\text{C}(\nu_\mu, \mu^-)$ reaction (a) and $^{12}\text{C}(\nu_e, e^-)$ (b) as a function of energy loss for a neutrino energy of $E_\nu = 180$ MeV, a momentum-transfer of $|\mathbf{q}| = 210$ MeV, and a Fermi momentum of $k_F = 225$ MeV.

FIG. 2. Angle-integrated cross section for the $^{12}\text{C}(\nu_\mu, \mu^-)$ reaction folded over the LSND neutrino spectrum as a function of the outgoing muon energy. A Fermi momentum of $k_F = 225$ MeV was used to simulate ^{12}C .

TABLES

TABLE I. $^{12}\text{C}(\nu_\mu, \mu^-)$ cross sections integrated over energy loss for an incoming neutrino energy of $E_\nu = 180$ MeV and a momentum transfer of $|\mathbf{q}| = 210$ MeV. All cross sections are reported relative to the free Fermi-gas (impulse with M) value using a Fermi momentum of $k_F = 225$ MeV. (The numbers below are the areas under the curves in Fig. 1 relative to the area under the impulse (M) curve.) Quantities in parentheses are the appropriate cross sections for the $^{12}\text{C}(\nu_e, e^-)$ reaction. The area under the impulse M curve of ν_μ (ν_e) is $5.213 \times 10^{-15} \text{ fm}^2$ ($8.115 \times 10^{-15} \text{ fm}^2$).

M^*/M	Impulse	RPA(I)	RPA (II)
1.00	1.00 (1.00)	0.56 (0.64)	—
0.68	0.70 (0.84)	0.36 (0.57)	0.53 (0.71)

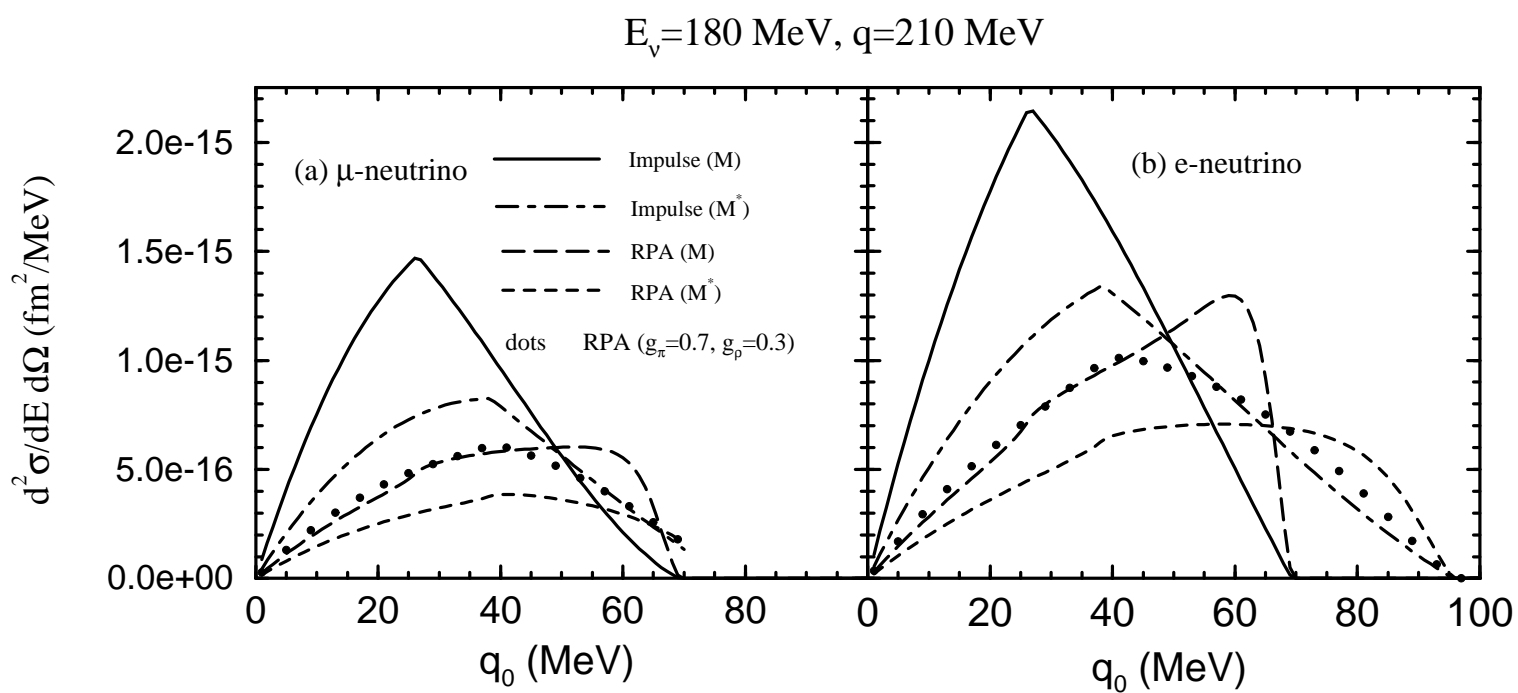


Fig. 1

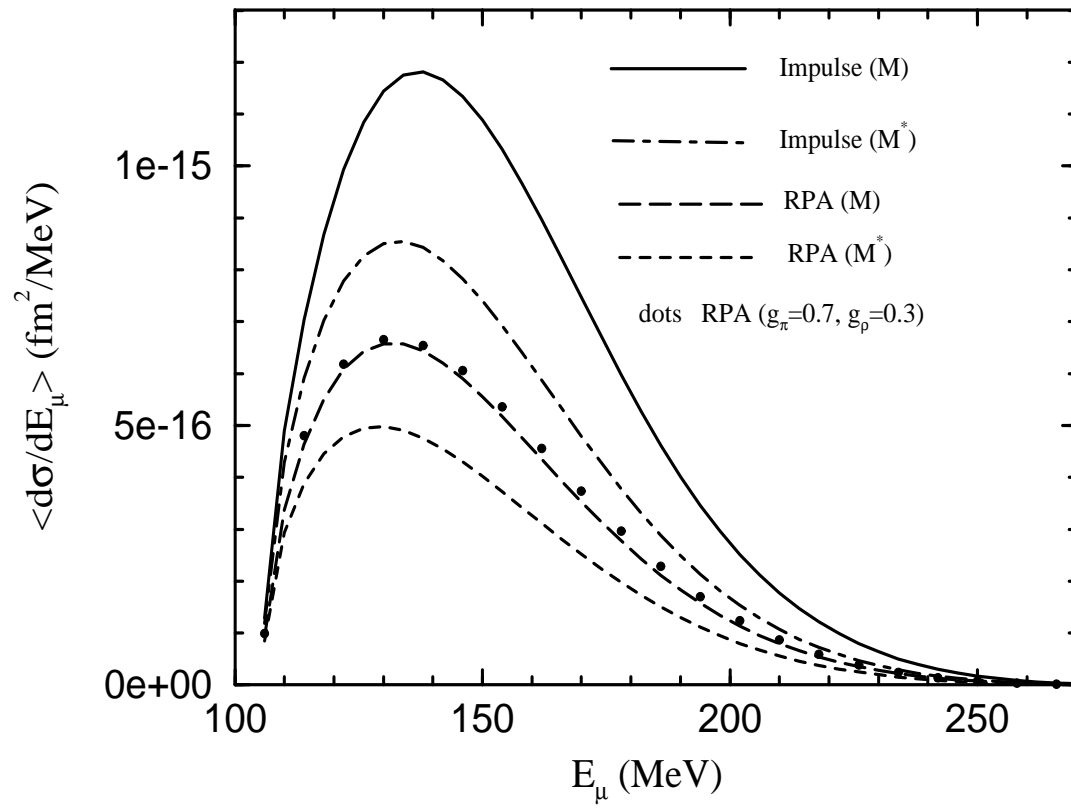


Fig. 2